Journal of Alzheimer's Disease xx (20xx) x–xx
DOI 10.3233/JAD-180395
IOS Press

Short-Term Effects of Microglia-Specific Mitochondrial Dysfunction on Amyloidosis in Transgenic Models of Alzheimer's Disease

Johannes Steffen[a,c,1], Jan Stenzel[a,1,2], Saleh Ibrahim[c] and Jens Pahnke[a,b,c,d,*]
[a]*Department of Neurology, University of Rostock, Neurodegeneration Research Lab (NRL), Germany*
[b]*Department of Neuro-/Pathology, University of Oslo (UiO) and Oslo University Hospital (OUS), Oslo, Norway*
[c]*University of Lübeck (UzL), LIED, Lübeck, Germany*
[d]*Department of Pharmacology, University of Latvia, Rīga, Latvia*

Accepted 28 June 2018

Abstract. Reduction of mitochondrial activity is a subtle and early event in the pathogenesis of Alzheimer's disease. Mitochondrial damage and consequentially enhanced production of reactive oxygen species is particularly occurring in the vicinity of amyloid plaques. Since all cells are affected by mitochondrial damage, analyses of cell type-specific effects are challenging. To study the impact of mitochondrial alterations on microglial activity in a homogeneous genetic background, we generated bone marrow chimeras of irradiated 46-days-old APP-transgenic mice. For reconstitution, bone marrow from CX3CR1-eGFP mice with mitochondria of either non-obese diabetic or C57BL/6J animals was utilized. Successful reconstitution was evident in 100-day-old animals, by the presence of eGFP-positive cells in liver and spleen. In the brain, one-third of IBA1-positive microglia cells were newly recruited eGFP-expressing cells. Although donor-derived microglia were equally located in the proximity of amyloid plaques, no difference was observed in either the amyloid level, total number, or microglial coverage of plaques. These results indicate that during this brief and early phase of amyloid deposition, beneficial mitochondrial alterations in the newly recruited third of microglial cells were not sufficient to affect the amyloidosis in APP-transgenic mice.

Keywords: Alzheimer's disease, amyloid-β, bone marrow cells, CX3CR1, microglia, neurodegenerative diseases, neuropathology, rodent models, spleen

INTRODUCTION

Alzheimer's disease (AD) is a chronic and progressive neurodegenerative amyloidosis. Histopathologically, it is characterized by extracellular deposition of amyloid-β (Aβ) and intracellular accumulation of hyperphosphorylated tau [1]. The extracellular plaques consist primarily of the 42-amino-acid-long isoform of Aβ [2], derived by proteolytic processing of the amyloid-β protein precursor (AβPP) [3]. The accumulation of monomeric Aβ leads to the generation of small soluble oligomers which further aggregate into larger insoluble fibrils [4] that also activate microglial cells [5]. It was long perceived that amyloid plaques are surrounded by reactive microglia; however, their specific role during disease progression is ambiguous and therefore still a matter of debate. The more recent identification of

[1]These authors contributed equally to this work.

[2]Current address: Core Facility Multimodal Small Animal Imaging, University of Rostock, Germany.

*Correspondence to: Jens Pahnke, University of Oslo, Department of Pathology (PAT), Translational Neurodegeneration Research and Neuropathology Lab, Postboks 4950 Nydalen, 0424 Oslo, Norway. Tel.: +47 230 71466; E-mail: jens.pahnke@medisin.uio.no.

ISSN 1387-2877/18/$35.00

various risk factors related to microglial function, like TREM2 [6–8], TYROBP [9, 10], CD33 [11], TLR4 [12], PGRN [13], or INPP5D [14] in genome-wide association studies further emphasized their impact on disease progression. In the early stages of the AD, microglia fulfill a beneficial role by eliminating soluble [15] and fibrillary forms of Aβ [16]. In this phase, further unspecific activation by lipopolysaccharide decreases plaque burden [17], while an impaired recruitment caused by the loss of the chemokine (C-C motif) receptor 2 (CCR2) accelerates the pathologic progression [18, 19].

On the other hand, it is equally established that the chronic activation of microglia is aggravating. Once activated, cellular functions are shifted to release cytotoxic factors like reactive oxygen species (ROS) [20], nitric monoxide (NO) [21], and tumor necrosis factor-α (TNF-α) [22]. Interruption of the proinflammatory IL-12/IL-23 pathway by genetic ablation resulted in decreased amyloid burden in transgenic AD mice [23]. The detrimental effects of chronic activation are supported by epidemiologic studies revealing that usage of nonsteroidal anti-inflammatory drugs (NSAIDs) decreased the incidence of AD [24]. Rapamycin, an immunosuppressant that diminished microglial activation but increased autophagy and degradation of Aβ, was able to reduce amyloid burden and prevent memory decline in a mouse model of AD [25]. A fundamental, yet crucial factor for an adequate microglial function is sufficient energy supply by mitochondrial activity. Analyses of postmortem AD brains revealed impaired activities of key enzymes of the Krebs cycle (pyruvate dehydrogenase complex, α-ketoglutarate dehydrogenase complex, isocitrate dehydrogenase) [26] and the cytochrome c oxidase (COX, complex IV) of the electron transport chain [27]. It is therefore supposed that mitochondrial insufficiencies significantly contribute to the pathophysiology of AD. We previously analyzed conplastic mice on the C57BL/6J background containing the mitochondria of common inbred mice strains (C57BL/6J, AKR/J, FVB/NJ, NOD/LtJ). Mitochondrial deviations in these mice led to significant differences in microglial response and Aβ load [28]. Mice with NOD/LtJ mitochondria had the highest levels of ATP, elevated microglial response with enhanced phagocytotic activity, and the lowest amyloid burden [28]. To further analyze the impact of mitochondrial alterations on microglial activity in a uniform genetic background, we created bone marrow chimeras using the well-established method of lethal irradiation and bone marrow reconstitution [29].

MATERIALS AND METHODS

Animals

Inbred C57BL/6 mice (B6) were purchased from the Jackson Laboratory (JAX stock #000664) and used as background strain. Mice expressing mutated human amyloid precursor protein (APP KM670/671NL) and mutated human presenilin 1 (PSL166P) controlled by the Thy1-promotor were provided by the University of Tübingen (Germany) and are referred to as 'hAPPtg' mice [30]. Non-obese diabetic (NOD/LtJ) mice were acquired from the Jackson Laboratory (JAX stock #001976). NOD/LtJ mice have three variations compared to B6 mice, in cytochrome c oxidase III (G > A at position 9348), NADH dehydrogenase 3 (T > C at position 9461), and mitochondrial tRNA arginine (A > AAA at position 9828) [28]. Mice with the C57BL/6J background (B6) and mitochondria of the NOD/LtJ strain were generated by mating female NOD/LtJ and male C57BL/6J mice for at least 9 generations and are referred to as B6-mt^{NOD} [31]. CX3CR1/eGFP mice were purchased from the Jackson Laboratory (JAX stock #005582) and have previously been described as fertile and devoid of developmental deficits [32]. CX3CR1/eGFP-mt^{NOD} and CX3CR1/eGFP-mt^{B6} were generated by mating male CX3CR1/eGFP mice with female B6-mt^{NOD} or B6 mice, respectively. All mice were housed in 12-h day/night cycles at 22°C with free access to food and water. All experiments were approved and carried out according to the local animal ethics committee.

Isolation of primary bone marrow cells

Required bone marrow cells were isolated from six to eight weeks old CX3CR1/eGFP-mt^{NOD} or CX3CR1/eGFP-mt^{B6} mice. After cervical dislocation, femur and tibia were removed, epi- and metaphyses were cut off, and bone marrow was flushed into a 50 mL tube using a 25-gauge needle and 5 mL medium (DMEM supplemented with 10% (v/v) FCS, 1% (v/v) GlutaMAX™, 1% (v/v) Penicillin-Streptomycin). Cells were centrifuged (10 min, 150 g, 4°C), resuspended in 50 mL medium and counted using a Fuchs-Rosenthal chamber. Cells were centrifuged again (10 min; 150 g; 4°C)

and resuspended in PBS to a final concentration of $6 \times 10^4/\mu L$.

Immunohistochemistry

Immunohistochemistry was performed as previously described [33–37]. In brief, mice were sacrificed by cervical dislocation and subsequently perfused with 20 mL of phosphate-buffered saline (PBS; pH 7.4). One hemisphere was immediately snap-frozen in liquid nitrogen and stored at –80°C, the second hemisphere was transferred to 4% buffered paraformaldehyde (PFA) and fixed overnight. Paraffin-embedded, 4 μm-thick coronal sections were deparaffinized and stained using hematoxylin and eosin (H&E). Immunohistochemical staining was performed using Bond-Max™ (Leica Biosystems GmbH/Menarini; Germany) automated staining system. Antibodies against ionized calcium-binding adapter molecule 1 (IBA1; 1:1000; Wako 019-19741; Germany) and β-Amyloid (6F3D; 1:200; DAKO M0872; Germany) were used. Slides were developed using Bond™ Polymer Refine Detection kit (Menarini/Leica; Germany) and digitized using MIRAX MIDI Scanner (Zeiss MicroImaging GmbH; Germany).

Plaque number and microglial coverage of plaques

Digitized slides were semi-automatically analyzed using the AxioVision software (Zeiss Microimaging GmbH, Germany) as previously described in [35]. In short, cortical regions of interest (ROIs) were initially defined and microglia and plaques were detected and separated based on their RGB color profile. The resulting binary images were automatically processed, plaque number and sizes were quantified and a rectangle was placed around each plaque. Finally, the microglial area within the rectangle was calculated and obtained data was exported for normalization and further analysis. For quantification, $n \geq 5$ animals of both sexes, and $n \geq 4$ sections per animal were analyzed.

Immunofluorescence

Brains were harvested as described above. PFA-fixed hemispheres were consecutively immersed in 15% and 25% sucrose solution and incubated for 12 h each, to remove PFA. Whole brains were mounted and frozen in cryo media (OCT Compound; Tissue Tek). 16 μm coronal sections within a specific range (bregma –1.5 mm to bregma –2.2 mm) were cut (Leica CM3050S). Slices were washed three times with PBS and blocked for one hour in blocking buffer (PBS supplemented with 5% goat serum and 0.5% Triton X-100). Sections were then incubated free-floating using primary antibodies against IBA1 (1:500; Wako 019-19741; Germany) and Aβ (6E10; 1:500; Covance SIG-39320; Germany) for 90 min in blocking buffer at 4°C. Afterward, slices were incubated using fluorescence-labeled secondary antibodies (1:500 anti-rabbit Cy3; 1:500 anti-mouse Cy3; Dianova; Germany) for 60 min and counterstained for 10 s using DAPI (1μg/mL). Slides were finally covered using DePex (Serva Electrophoresis; Germany), visualized using a Zeiss LSM 700 microscope (Carl Zeiss; Germany) and analyzed using ZEN 2 software (Carl Zeiss; Germany). IBA1-positive and eGFP-positive cells were counted in isocortical region A (retrosplenial area, posterior parietal association areas, primary somatosensory area, and auditory areas), isocortical region B (temporal association areas, ecto- and perirhinal areas), hippocampus and brain stem ($n \geq 1500$ $IBA1^+$ cells per animal, $n \geq 3$ sections per animal, $n \geq 4$ animals of both sexes per group).

Enzyme-linked immunosorbent assay (ELISA)

Measurement of $A\beta_{42}$ concentration in whole brain homogenates was performed as described previously [33]. Briefly, snap-frozen hemispheres without cerebellum and brain stem were slowly thawed on ice and homogenized using a PreCellys24 (12 s; 6,000 rpm). Homogenate was mixed with 50 volumes of carbonate buffer (1 M sodium carbonate, 50 mM sodium chloride, pH 11.5, supplemented with protease inhibitors (cOmplete mini, Roche Diagnostics International AG, Switzerland) using PreCellys24 (5 s; 5,000 rpm) and subsequently centrifuged (90 min, 24,000 g, 4°C) to separate soluble and insoluble Aβ-species. The supernatant (buffer-soluble fraction) was mixed with 1.6 volumes guanidine hydrochloride buffer (8.2 M guanidine hydrochloride, 82 mM Tris, pH 8.0). Protein content was measured using a Nanodrop1000 device (Thermo Fisher Scientific; USA). ELISA (hAmyloid β42 ELISA, TK42HS, The Genetics Company (TGC), Schlieren, Switzerland) was performed according to the manufacturer's instructions.

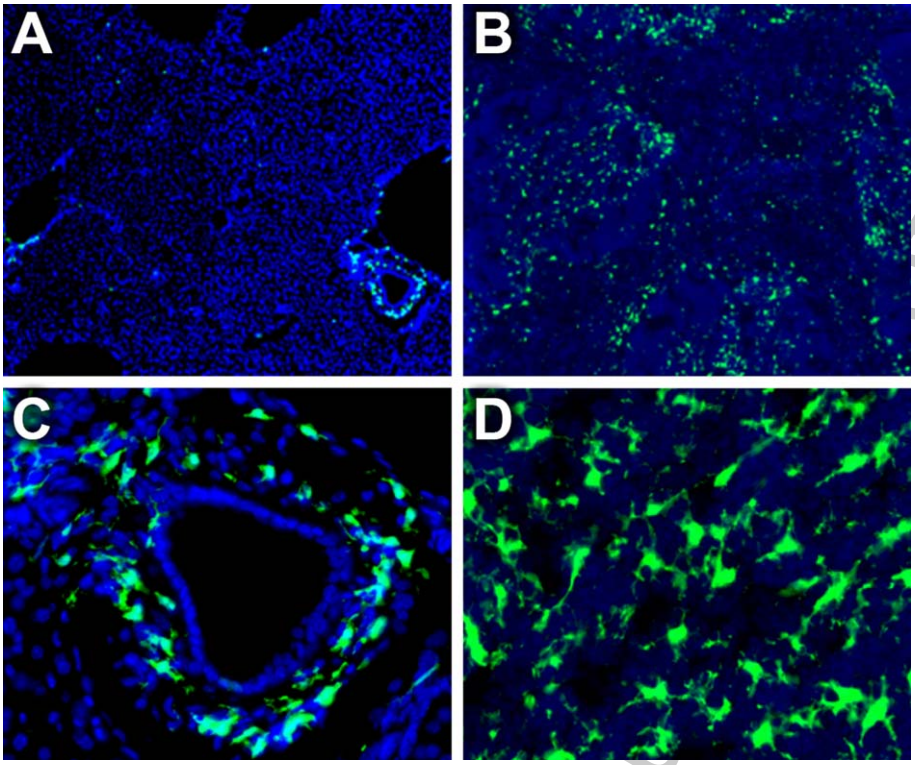

Fig. 1. Transplanted hematopoietic stem cells yield immune cells migrating to liver and spleen. An overview of the liver shows migrated, green fluorescent cells which originated from transplanted bone marrow (A). The magnified section (C) presents a central vessel encircled by eGFP-positive cells. The overview (B) and a magnified section (D) of the spleen revealed an even distribution of green fluorescent cells. (Magnification in A, B: 10x; C, D: 40x).

Statistical analysis

Results were statistically analyzed using unpaired *t*-test in GraphPad Prism 6 (GraphPad Software Inc., USA) and considered significant for $p \leq 0.05$. Data are presented as arithmetic mean with the corresponding standard error of the mean (SEM).

RESULTS

Generation of an AD-model with mitochondrial alterations restricted to microglia

To generate animals with the NOD- (NOD/LtJ) or B6-derived (C57BL/6J) mitochondria and microglia specific eGFP-expression, C57BL/6J-mt^{B6} and previously described conplastic C57BL/6J-mt^{NOD} [28] females were mated with male CX3CR1/eGFP mice. Next, hAPPtg mice were lethally irradiated (two times with 9 Gy and a 4-h pause using a ^{137}Cs source) at the age of 45 days ($n \geq 5$ animal per group). After 24 h, 6×10^6 isolated bone marrow cells were transplanted via the tail vein. Six- to eight-weeks-old CX3CR1/eGFP-mt^{NOD} or CX3CR1/eGFP-mt^{B6} mice acted as donors. To confirm the efficiency of the bone marrow reconstitution, liver and spleen of 100-days-old mice were analyzed using immunofluorescence microscopy. Green-fluorescent cells were present in liver and spleen (Fig. 1), indicating a successful transplantation of hematopoietic stem cells. Furthermore, green fluorescent cells resembling microglia in size and shape were evident in different parts of the brain, including isocortex, hippocampus, and brain stem (Fig. 2). Immunofluorescent stains against microglial maker IBA1 confirmed this assumption and displayed the expected double fluorescent microglia (Fig. 3). Quantification of IBA1-positive cells revealed a similar percentage of IBA1$^+$ eGFP$^+$ cells in the brains (mt^{NOD}: 35%; mt^{B6}: 37%). Donor-derived microglial cells were located in the immediate surrounding of amyloid plaques (Fig. 4). In sum, these results indicate the successful generation of an amyloidosis (AD) mouse model with specific mitochondrial deviations,

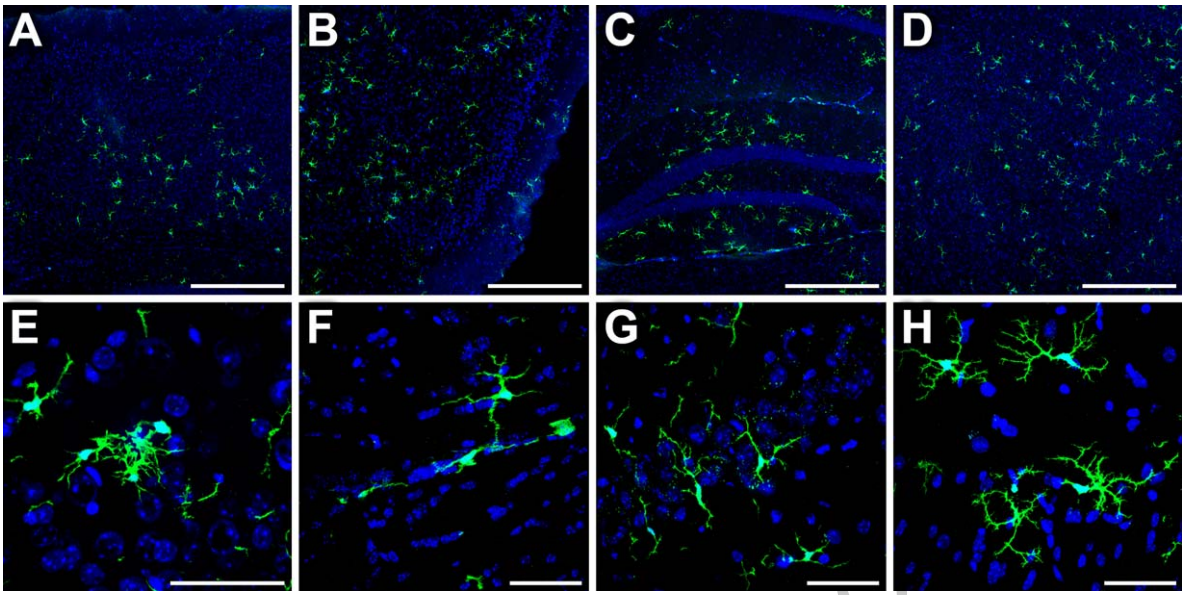

Fig. 2. Newly recruited green fluorescent labeled cells populate different brain regions. Overviews of (A) isocortical area, representing retrosplenial, posterior parietal association, primary somatosensory, and auditory areas, (B) isocortical area, representing temporal association-, ecto-, and perirhinal areas, (C) hippocampus, and (D) brain stem, representing thalamus and hypothalamus, revealed the consistent presence of eGFP-positive cells in different brain regions. Corresponding higher magnifications (E-H) demonstrate that green fluorescent cells resemble microglia in size and shape. (Scale bars: A–D: 400 μm; E - H: 50 μm).

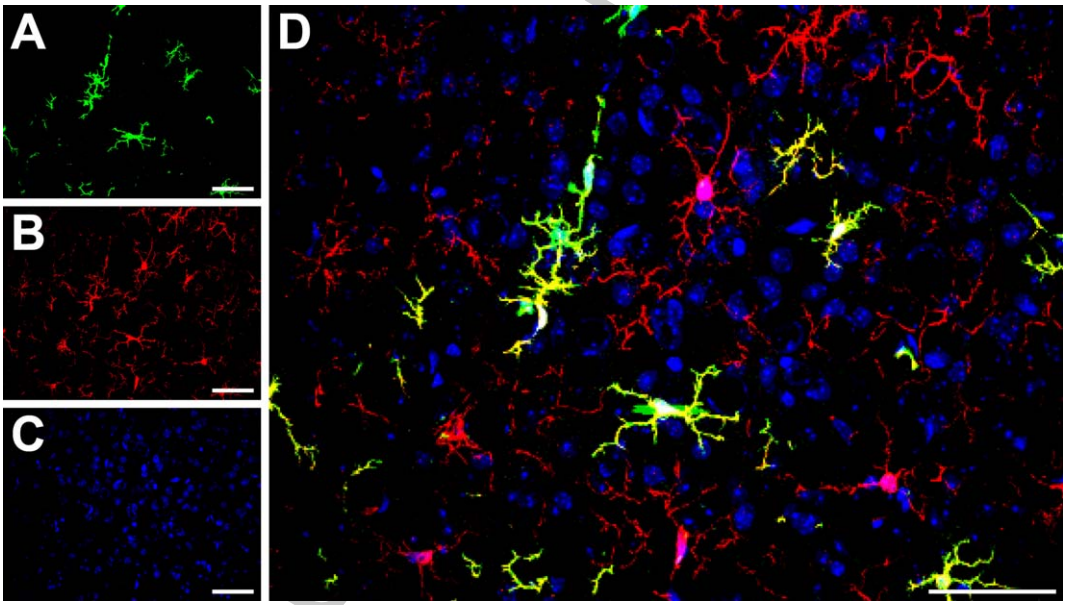

Fig. 3. Microglia cells in the brain of bone marrow transplanted mice. (D) Merged picture of donor bone marrow-derived GFP-positive cells (A, green), IBA1 stained microglial cells (B, red) with nuclear counterstain (C, blue) shows resident microglia of acceptor animal (only $IBA1^+$, red) and donor-derived, newly recruited microglial cells (IBA^+ and $eGFP^+$, green-yellow) in the cortex of bone marrow transplanted mice. (Scale bars: 50 μm).

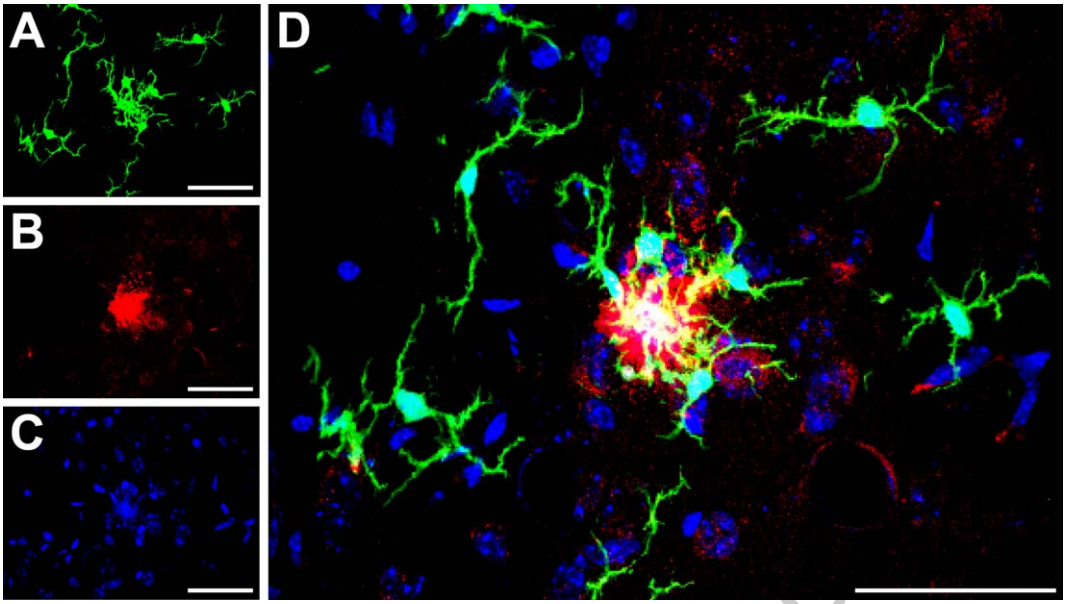

Fig. 4. Recruited microglia are in close proximity to amyloid depositions. D) Merged picture of donor bone marrow-derived GFP-positive cells (A, green), 6E10 stained amyloid plaque (B, red) with nuclear counterstain (C, blue) demonstrates that donor-derived microglial cells are recruited to the brain and interact with amyloid plaques. (Scale bars: 50 μm).

limited to hematopoietic system. In the brain, these alterations are restricted to newly recruited microglial cells.

Impact of mitochondrial alterations on microglial activity

Acceptor mice with transplanted, mitochondrial NOD-type bone marrow (hAPPtg-CX3CR1/eGFP-mt^{NOD}) were analyzed at 100 days of age. Chimeric B6-type mice (hAPPtg-CX3CR1/eGFP-mt^{B6}) with transplanted mitochondrial B6-type bone marrow served as controls. Cortical amyloidosis and microglial activation were analyzed in both groups using semi-automated analysis of digital slides (as previously described [35]). The mean plaque number per 10 mm^2 was on a similar level (Fig. 5) in mt^{B6} (212 Plaques/10 mm^2) and mt^{NOD} (223 Plaques/10 mm^2) transplanted animals. The average size of individual plaques and accordingly the cortical area covered by amyloid plaques were not changed in chimeric animals with mt^{NOD} microglia. ELISA quantification further revealed a similar concentration of soluble $A\beta_{42}$. Finally, activation and recruitment of microglia were likewise not significantly changed, as microglial coverage of plaques was at a similar level in both groups (Fig. 5).

DISCUSSION

Reduced energy metabolism [38] and mitochondrial activity [39] are early, precedent events in the pathogenesis of AD and risk factors for early onset and accelerated progression [40]. Mitochondrial alterations occur particularly in the vicinity of amyloid plaques [41]. These dysfunctional mitochondria become key targets of the autophagic degradation in AD [42], entailing a declined number of mitochondria [43] and increased levels of ROS in the course of the disease [44]. Finally, ROS is sufficient to boost generation of Aβ [44], closing the vicious circle of mitochondrial dysfunction, ROS production, and Aβ formation. As mitochondrial activities are absolutely fundamental, consequences of an impaired function are diverse and detrimental. In microglia, defective mitochondrial function and elevated levels of ROS contribute to the polarization to an M(1) phenotype [45], activation of NFκB and MAPK signaling and increased expression of various pro-inflammatory mediators [46, 47]. However, a reasonably distinction of mitochondrial effects in distinct cell types was so far most challenging.

Here, we introduced a model in which mitochondrial alterations in the brain are limited to microglial cells. These cells are easily recognizable by their exclusive expression of eGFP, achieved by

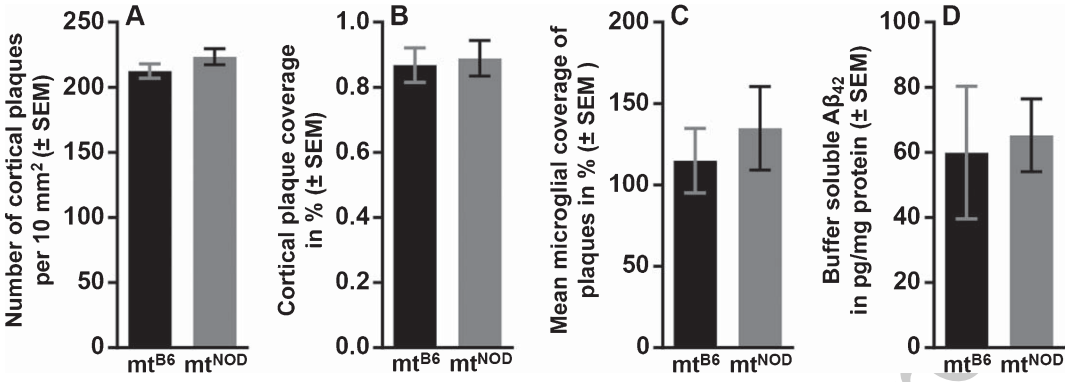

Fig. 5. Cortical amyloidosis and microglial activation is unchanged in bone marrow chimeric mice. The number of cortical plaques (A) and cortical plaque coverage (B) were at a similar level. Furthermore, microglial coverage of plaques (C) and levels of buffer-soluble $A\beta_{42}$ (D) revealed no significant differences between mice transplanted with either mt^{NOD} or mt^{B6} bone marrow. (Unpaired *t*-test displayed no significant differences, $n \geq 4$ animals per group, $n \geq 3$ sections per animal).

replacement of the fractalkine receptor (chemokine (C-X3-C motif) receptor 1; CX3CR1) by eGFP [32]. The newly recruited microglia derived from transplanted heterozygous bone marrow cells, functionally co-express eGFP and CX3CR1 [32]. Therefore, the suspected involvement of CX3CR1 in microglial clearance of Aβ in a gene dose-dependent manner has to be considered in interpreting the results. In 3xTg-AD mice, knockout the fractalkine receptor ameliorated neuronal loss while Aβ levels and microglial phagocytosis activity were unchanged [48]. In contrast, Lee et al. [49] demonstrated that CX3CR1-deficiency alters microglial activation. While CX3CR1-deficient animals presented with fewer microglia in the vicinity of plaques and reduced deposition of Aβ, heterozygous animals exhibited an intermediate phenotype [49]. Since phagocytic capacity is increased in CX3CR1-deficient microglia [49–51], the newly recruited microglia might rather be characterized by an amplified phagocytic activity compared to wild-type cells with natural CX3CR1-expression.

Although the newly recruited microglia harboring mitochondrial alterations were found in the vicinity of plaques, they had no significant effect on amyloid deposition at the evaluated age of 100 days. The microglial coverage of plaques was likewise unchanged. In contrast, conplastic APP-B6xmtNOD mice have previously been described with reduced number and size of plaques and enhanced microglial coverage starting at 100 days of age [28]. Therefore, the introduced mitochondrial alterations in microglial cells do not seem to immediately interfere with amyloid deposition in APP-transgenic mice. However, in the formerly analyzed models, mitochondrial alterations affected all cell-types, including those that likewise play crucial roles in amyloid elimination, like astrocytes [52, 53], pericytes [54–56], and endothelial cells [33, 54, 56]. Furthermore, at 100 days of age, only a third (35%) of the microglial cells originated from the transplanted mt^{NOD} bone marrow, providing another possible explanation for the minimal impact of mt^{NOD} microglial cells. Since mt^{NOD} microglia were shown to have a higher phagocytic activity *in vitro* and reduced Aβ-levels *in vivo* [28], the induction of an increased microglial turnover, e.g., by specific ablation [57, 58], and expanded observation periods will provide an advantageous approach to reveal the full potential of the microglia-specific alterations in AD in the future.

ACKNOWLEDGMENTS

The experiments were performed at the University of Rostock / Department of Neurology and financed by the intramural grant of the University of Rostock (FORUN 889012) to Ja.S. We thank Thomas Brüning for technical support with histology and Gerda Brüsch for help with animals.

The work of J.P. is/was supported by the following grants: Deutsche Forschungsgemeinschaft/ Germany (DFG PA930/9, DFG PA930/12); Leibniz Society/ Germany (SAW-2015-IPB-2); HelseSØ/ Norway (2016062); Norsk forskningsrådet/ Norway (247179, 251290, 260786); Horizon 2020/ European Union (643417 (PROP-AD)).

NeuroGeM is an EU Joint Programme - Neurodegenerative Disease Research (JPND) project. The project is supported through the following funding organizations under the aegis of JPND - www.jpnd.eu

(CIHR – Canada, BMBF – Germany, NRF #247179 – Norway, ZonMW – The Netherlands).

PROP-AD is an EU Joint Programme - Neurodegenerative Disease Research (JPND) project. The project is supported through the following funding organizations under the aegis of JPND - www.jpnd.eu (AKA #301228 – Finland, BMBF #01ED1605-Germany, CSO-MOH #30000-12631 - Israel, NFR #260786 - Norway, SRC #2015-06795 - Sweden). This project has received funding from the European Union's Horizon 2020 research and innovation programme under grant agreement #643417 (JPcofuND).

Authors' disclosures available online (https://www.j-alz.com/manuscript-disclosures/18-0395r1).

REFERENCES

[1] Suh YH, Checler F (2002) Amyloid precursor protein, presenilins, and alpha-synuclein: Molecular pathogenesis and pharmacological applications in Alzheimer's disease. *Pharmacol Rev* **54**, 469-525.

[2] Glenner GG, Wong CW (1984) Alzheimer's disease and Down's syndrome: Sharing of a unique cerebrovascular amyloid fibril protein. *Biochem Biophys Res Commun* **122**, 1131-1135.

[3] Haass C, De Strooper B (1999) The presenilins in Alzheimer's disease–proteolysis holds the key. *Science* **286**, 916-919.

[4] Aleksis R, Oleskovs F, Jaudzems K, Pahnke J, Biverstal H (2017) Structural studies of amyloid-beta peptides: Unlocking the mechanism of aggregation and the associated toxicity. *Biochimie* **140**, 176-192.

[5] Doens D, Fernandez PL (2014) Microglia receptors and their implications in the response to amyloid beta for Alzheimer's disease pathogenesis. *J Neuroinflammation* **11**, 48.

[6] Fenoglio C, Galimberti D, Piccio L, Scalabrini D, Panina P, Buonsanti C, Venturelli E, Lovati C, Forloni G, Mariani C, Bresolin N, Scarpini E (2007) Absence of TREM2 polymorphisms in patients with Alzheimer's disease and Frontotemporal Lobar Degeneration. *Neurosci Lett* **411**, 133-137.

[7] Cuyvers E, Bettens K, Philtjens S, Van Langenhove T, Gijselinck I, van der Zee J, Engelborghs S, Vandenbulcke M, Van Dongen J, Geerts N, Maes G, Mattheijssens M, Peeters K, Cras P, Vandenberghe R, De Deyn PP, Van Broeckhoven C, Cruts M, Sleegers K, consortium B (2014) Investigating the role of rare heterozygous TREM2 variants in Alzheimer's disease and frontotemporal dementia. *Neurobiol Aging* **35**, 726 e711-729.

[8] Benitez BA, Cooper B, Pastor P, Jin SC, Lorenzo E, Cervantes S, Cruchaga C (2013) TREM2 is associated with the risk of Alzheimer's disease in Spanish population. *Neurobiol Aging* **34**, 1711 e1715-1717.

[9] Zhang B, Gaiteri C, Bodea LG, Wang Z, McElwee J, Podtelezhnikov AA, Zhang C, Xie T, Tran L, Dobrin R, Fluder E, Clurman B, Melquist S, Narayanan M, Suver C, Shah H, Mahajan M, Gillis T, Mysore J, MacDonald ME, Lamb JR, Bennett DA, Molony C, Stone DJ, Gudnason V, Myers AJ, Schadt EE, Neumann H, Zhu J, Emilsson V (2013) Integrated systems approach identifies genetic nodes and networks in late-onset Alzheimer's disease. *Cell* **153**, 707-720.

[10] Ma J, Jiang T, Tan L, Yu JT (2015) TYROBP in Alzheimer's disease. *Mol Neurobiol* **51**, 820-826.

[11] Malik M, Simpson JF, Parikh I, Wilfred BR, Fardo DW, Nelson PT, Estus S (2013) CD33 Alzheimer's risk-altering polymorphism, CD33 expression, and exon 2 splicing. *J Neurosci* **33**, 13320-13325.

[12] Song M, Jin J, Lim JE, Kou J, Pattanayak A, Rehman JA, Kim HD, Tahara K, Lalonde R, Fukuchi K (2011) TLR4 mutation reduces microglial activation, increases Abeta deposits and exacerbates cognitive deficits in a mouse model of Alzheimer's disease. *J Neuroinflammation* **8**, 92.

[13] Minami SS, Min SW, Krabbe G, Wang C, Zhou Y, Asgarov R, Li Y, Martens LH, Elia LP, Ward ME, Mucke L, Farese RV, Jr., Gan L (2014) Progranulin protects against amyloid beta deposition and toxicity in Alzheimer's disease mouse models. *Nat Med* **20**, 1157-1164.

[14] Lambert JC, Ibrahim-Verbaas CA, Harold D, Naj AC, Sims R, Bellenguez C, DeStafano AL, Bis JC, Beecham GW, Grenier-Boley B, Russo G, Thorton-Wells TA, Jones N, Smith AV, Chouraki V, Thomas C, Ikram MA, Zelenika D, Vardarajan BN, Kamatani Y, Lin CF, Gerrish A, Schmidt H, Kunkle B, Dunstan ML, Ruiz A, Bihoreau MT, Choi SH, Reitz C, Pasquier F, Cruchaga C, Craig D, Amin N, Berr C, Lopez OL, De Jager PL, Deramecourt V, Johnston JA, Evans D, Lovestone S, Letenneur L, Moron FJ, Rubinsztein DC, Eiriksdottir G, Sleegers K, Goate AM, Fievet N, Huentelman MW, Gill M, Brown K, Kamboh MI, Keller L, Barberger-Gateau P, McGuiness B, Larson EB, Green R, Myers AJ, Dufouil C, Todd S, Wallon D, Love S, Rogaeva E, Gallacher J, St George-Hyslop P, Clarimon J, Lleo A, Bayer A, Tsuang DW, Yu L, Tsolaki M, Bossu P, Spalletta G, Proitsi P, Collinge J, Sorbi S, Sanchez-Garcia F, Fox NC, Hardy J, Deniz Naranjo MC, Bosco P, Clarke R, Brayne C, Galimberti D, Mancuso M, Matthews F, European Alzheimer's Disease Initiative (EADI); Genetic and Environmental Risk in Alzheimer's Disease; Alzheimer's Disease Genetic Consortium; Cohorts for Heart and Aging Research in Genomic Epidemiology, Moebus S, Mecocci P, Del Zompo M, Maier W, Hampel H, Pilotto A, Bullido M, Panza F, Caffarra P, Nacmias B, Gilbert JR, Mayhaus M, Lannefelt L, Hakonarson H, Pichler S, Carrasquillo MM, Ingelsson M, Beekly D, Alvarez V, Zou F, Valladares O, Younkin SG, Coto E, Hamilton-Nelson KL, Gu W, Razquin C, Pastor P, Mateo I, Owen MJ, Faber KM, Jonsson PV, Combarros O, O'Donovan MC, Cantwell LB, Soininen H, Blacker D, Mead S, Mosley TH Jr, Bennett DA, Harris TB, Fratiglioni L, Holmes C, de Bruijn RF, Passmore P, Montine TJ, Bettens K, Rotter JI, Brice A, Morgan K, Foroud TM, Kukull WA, Hannequin D, Powell JF, Nalls MA, Ritchie K, Lunetta KL, Kauwe JS, Boerwinkle E, Riemenschneider M, Boada M, Hiltuenen M, Martin ER, Schmidt R, Rujescu D, Wang LS, Dartigues JF, Mayeux R, Tzourio C, Hofman A, Nothen MM, Graff C, Psaty BM, Jones L, Haines JL, Holmans PA, Lathrop M, Pericak-Vance MA, Launer LJ, Farrer LA, van Duijn CM, Van Broeckhoven C, Moskvina V, Seshadri S, Williams J, Schellenberg GD, Amouyel P (2013) Meta-analysis of 74,046 individuals identifies 11 new susceptibility loci for Alzheimer's disease. *Nat Genet* **45**, 1452-1458.

[15] Mandrekar S, Jiang Q, Lee CY, Koenigsknecht-Talboo J, Holtzman DM, Landreth GE (2009) Microglia mediate the clearance of soluble Abeta through fluid phase macropinocytosis. *J Neurosci* **29**, 4252-4262.

[16] Koenigsknecht J, Landreth G (2004) Microglial phagocytosis of fibrillar beta-amyloid through a beta1 integrin-dependent mechanism. *J Neurosci* **24**, 9838-9846.

[17] Herber DL, Mercer M, Roth LM, Symmonds K, Maloney J, Wilson N, Freeman MJ, Morgan D, Gordon MN (2007) Microglial activation is required for Abeta clearance after intracranial injection of lipopolysaccharide in APP transgenic mice. *J Neuroimmune Pharmacol* **2**, 222-231.

[18] El Khoury J, Toft M, Hickman SE, Means TK, Terada K, Geula C, Luster AD (2007) Ccr2 deficiency impairs microglial accumulation and accelerates progression of Alzheimer-like disease. *Nat Med* **13**, 432-438.

[19] Mildner A, Schlevogt B, Kierdorf K, Bottcher C, Erny D, Kummer MP, Quinn M, Bruck W, Bechmann I, Heneka MT, Priller J, Prinz M (2011) Distinct and non-redundant roles of microglia and myeloid subsets in mouse models of Alzheimer's disease. *J Neurosci* **31**, 11159-11171.

[20] Colton CA, Gilbert DL (1987) Production of superoxide anions by a CNS macrophage, the microglia. *FEBS Lett* **223**, 284-288.

[21] Boje KM, Arora PK (1992) Microglial-produced nitric oxide and reactive nitrogen oxides mediate neuronal cell death. *Brain Res* **587**, 250-256.

[22] Sawada M, Kondo N, Suzumura A, Marunouchi T (1989) Production of tumor necrosis factor-alpha by microglia and astrocytes in culture. *Brain Res* **491**, 394-397.

[23] Vom Berg J, Prokop S, Miller KR, Obst J, Kalin RE, Lopategui-Cabezas I, Wegner A, Mair F, Schipke CG, Peters O, Winter Y, Becher B, Heppner FL (2012) Inhibition of IL-12/IL-23 signaling reduces Alzheimer's disease-like pathology and cognitive decline. *Nat Med* **18**, 1812-1819.

[24] McGeer PL, Schulzer M, McGeer EG (1996) Arthritis and anti-inflammatory agents as possible protective factors for Alzheimer's disease: A review of 17 epidemiologic studies. *Neurology* **47**, 425-432.

[25] Richardson A, Galvan V, Lin AL, Oddo S (2015) How longevity research can lead to therapies for Alzheimer's disease: The rapamycin story. *Exp Gerontol* **68**, 51-58.

[26] Petrozzi L, Ricci G, Giglioli NJ, Siciliano G, Mancuso M (2007) Mitochondria and neurodegeneration. *Biosci Rep* **27**, 87-104.

[27] Gibson GE, Sheu KF, Blass JP (1998) Abnormalities of mitochondrial enzymes in Alzheimer disease. *J Neural Transm (Vienna)* **105**, 855-870.

[28] Scheffler K, Krohn M, Dunkelmann T, Stenzel J, Miroux B, Ibrahim S, von Bohlen Und Halbach O, Heinze HJ, Walker LC, Gsponer JA, Pahnke J (2012) Mitochondrial DNA polymorphisms specifically modify cerebral beta-amyloid proteostasis. *Acta Neuropathol* **124**, 199-208.

[29] Turrin NP, Plante MM, Lessard M, Rivest S (2007) Irradiation does not compromise or exacerbate the innate immune response in the brains of mice that were transplanted with bone marrow stem cells. *Stem Cells* **25**, 3165-3172.

[30] Radde R, Bolmont T, Kaeser SA, Coomaraswamy J, Lindau D, Stoltze L, Calhoun ME, Jaggi F, Wolburg H, Gengler S, Haass C, Ghetti B, Czech C, Holscher C, Mathews PM, Jucker M (2006) Abeta42-driven cerebral amyloidosis in transgenic mice reveals early and robust pathology. *EMBO Rep* **7**, 940-946.

[31] Yu X, Gimsa U, Wester-Rosenlof L, Kanitz E, Otten W, Kunz M, Ibrahim SM (2009) Dissecting the effects of mtDNA variations on complex traits using mouse conplastic strains. *Genome Res* **19**, 159-165.

[32] Jung S, Aliberti J, Graemmel P, Sunshine MJ, Kreutzberg GW, Sher A, Littman DR (2000) Analysis of fractalkine receptor CX(3)CR1 function by targeted deletion and green fluorescent protein reporter gene insertion. *Mol Cell Biol* **20**, 4106-4114.

[33] Krohn M, Lange C, Hofrichter J, Scheffler K, Stenzel J, Steffen J, Schumacher T, Bruning T, Plath AS, Alfen F, Schmidt A, Winter F, Rateitschak K, Wree A, Gsponer J, Walker LC, Pahnke J (2011) Cerebral amyloid-beta proteostasis is regulated by the membrane transport protein ABCC1 in mice. *J Clin Invest* **121**, 3924-3931.

[34] Schumacher T, Krohn M, Hofrichter J, Lange C, Stenzel J, Steffen J, Dunkelmann T, Paarmann K, Frohlich C, Uecker A, Plath AS, Sommer A, Bruning T, Heinze HJ, Pahnke J (2012) ABC transporters B1, C1 and G2 differentially regulate neuroregeneration in mice. *PLoS One* **7**, e35613.

[35] Scheffler K, Stenzel J, Krohn M, Lange C, Hofrichter J, Schumacher T, Bruning T, Plath AS, Walker L, Pahnke J (2011) Determination of spatial and temporal distribution of microglia by 230nm-high-resolution, high-throughput automated analysis reveals different amyloid plaque populations in an APP/PS1 mouse model of Alzheimer's disease. *Curr Alzheimer Res* **8**, 781-788.

[36] Frohlich C, Paarmann K, Steffen J, Stenzel J, Krohn M, Heinze HJ, Pahnke J (2013) Genomic background-related activation of microglia and reduced beta-amyloidosis in a mouse model of Alzheimer's disease. *Eur J Microbiol Immunol (Bp)* **3**, 21-27.

[37] Steffen J, Krohn M, Schwitlick C, Bruning T, Paarmann K, Pietrzik CU, Biverstal H, Jansone B, Langer O, Pahnke J (2017) Expression of endogenous mouse APP modulates beta-amyloid deposition in hAPP-transgenic mice. *Acta Neuropathol Commun* **5**, 49.

[38] Wang X, Wang W, Li L, Perry G, Lee HG, Zhu X (2014) Oxidative stress and mitochondrial dysfunction in Alzheimer's disease. *Biochim Biophys Acta* **1842**, 1240-1247.

[39] Maurer I, Zierz S, Moller HJ (2000) A selective defect of cytochrome c oxidase is present in brain of Alzheimer disease patients. *Neurobiol Aging* **21**, 455-462.

[40] Zhao W, Wang J, Varghese M, Ho L, Mazzola P, Haroutunian V, Katsel PL, Gibson GE, Levine S, Dubner L, Pasinetti GM (2015) Impaired mitochondrial energy metabolism as a novel risk factor for selective onset and progression of dementia in oldest-old subjects. *Neuropsychiatr Dis Treat* **11**, 565-574.

[41] Xie H, Guan J, Borrelli LA, Xu J, Serrano-Pozo A, Bacskai BJ (2013) Mitochondrial alterations near amyloid plaques in an Alzheimer's disease mouse model. *J Neurosci* **33**, 17042-17051.

[42] Moreira PI, Siedlak SL, Wang X, Santos MS, Oliveira CR, Tabaton M, Nunomura A, Szweda LI, Aliev G, Smith MA, Zhu X, Perry G (2007) Increased autophagic degradation of mitochondria in Alzheimer disease. *Autophagy* **3**, 614-615.

[43] Hirai K, Aliev G, Nunomura A, Fujioka H, Russell RL, Atwood CS, Johnson AB, Kress Y, Vinters HV, Tabaton M, Shimohama S, Cash AD, Siedlak SL, Harris PL, Jones PK, Petersen RB, Perry G, Smith MA (2001) Mitochondrial abnormalities in Alzheimer's disease. *J Neurosci* **21**, 3017-3023.

[44] Leuner K, Schutt T, Kurz C, Eckert SH, Schiller C, Occhipinti A, Mai S, Jendrach M, Eckert GP, Kruse SE, Palmiter RD, Brandt U, Drose S, Wittig I, Willem M, Haass C,

Reichert AS, Muller WE (2012) Mitochondrion-derived reactive oxygen species lead to enhanced amyloid beta formation. *Antioxid Redox Signal* **16**, 1421-1433.

[45] Bordt EA, Polster BM (2014) NADPH oxidase- and mitochondria-derived reactive oxygen species in proinflammatory microglial activation: A bipartisan affair? *Free Radic Biol Med* **76**, 34-46.

[46] Nakanishi H, Wu Z (2009) Microglia-aging: Roles of microglial lysosome- and mitochondria-derived reactive oxygen species in brain aging. *Behav Brain Res* **201**, 1-7.

[47] Park J, Choi H, Min JS, Park SJ, Kim JH, Park HJ, Kim B, Chae JI, Yim M, Lee DS (2013) Mitochondrial dynamics modulate the expression of pro-inflammatory mediators in microglial cells. *J Neurochem* **127**, 221-232.

[48] Fuhrmann M, Bittner T, Jung CK, Burgold S, Page RM, Mitteregger G, Haass C, LaFerla FM, Kretzschmar H, Herms J (2010) Microglial Cx3cr1 knockout prevents neuron loss in a mouse model of Alzheimer's disease. *Nat Neurosci* **13**, 411-413.

[49] Lee S, Varvel NH, Konerth ME, Xu G, Cardona AE, Ransohoff RM, Lamb BT (2010) CX3CR1 deficiency alters microglial activation and reduces beta-amyloid deposition in two Alzheimer's disease mouse models. *Am J Pathol* **177**, 2549-2562.

[50] Liu Z, Condello C, Schain A, Harb R, Grutzendler J (2010) CX3CR1 in microglia regulates brain amyloid deposition through selective protofibrillar amyloid-beta phagocytosis. *J Neurosci* **30**, 17091-17101.

[51] Zabel MK, Zhao L, Zhang Y, Gonzalez SR, Ma W, Wang X, Fariss RN, Wong WT (2016) Microglial phagocytosis and activation underlying photoreceptor degeneration is regulated by CX3CL1-CX3CR1 signaling in a mouse model of retinitis pigmentosa. *Glia* **64**, 1479-1491.

[52] Ries M, Sastre M (2016) Mechanisms of Abeta Clearance and Degradation by Glial Cells. *Front Aging Neurosci* **8**, 160.

[53] Acosta C, Anderson HD, Anderson CM (2017) Astrocyte dysfunction in Alzheimer disease. *J Neurosci Res* **95**, 2430-2447.

[54] Yamazaki Y, Kanekiyo T (2017) Blood-brain barrier dysfunction and the pathogenesis of Alzheimer's disease. *Int J Mol Sci* **18**, E1965.

[55] Winkler EA, Sagare AP, Zlokovic BV (2014) The pericyte: A forgotten cell type with important implications for Alzheimer's disease? *Brain Pathol* **24**, 371-386.

[56] Sweeney MD, Sagare AP, Zlokovic BV (2018) Blood-brain barrier breakdown in Alzheimer disease and other neurodegenerative disorders. *Nat Rev Neurol* **14**, 133-150.

[57] Spangenberg EE, Lee RJ, Najafi AR, Rice RA, Elmore MR, Blurton-Jones M, West BL, Green KN (2016) Eliminating microglia in Alzheimer's mice prevents neuronal loss without modulating amyloid-beta pathology. *Brain* **139**, 1265-1281.

[58] Dagher NN, Najafi AR, Kayala KM, Elmore MR, White TE, Medeiros R, West BL, Green KN (2015) Colony-stimulating factor 1 receptor inhibition prevents microglial plaque association and improves cognition in 3xTg-AD mice. *J Neuroinflammation* **12**, 139.